Analysis and combined optimization of the cladding layer in outcoupling-improved top emitting OLEDs

Ligong Yang (杨立功), Peng Wu (吴 鹏), Biqin Huang (黄弼勤), and Peifu Gu (顾培夫)

Department of Optical Engineering, Zhejiang University, Hangzhou 310027

Received October 31, 2003

Within the associated framework of metal-dielectric films optics and the dual-metal-mirror microcavity structure, the effect of a cladding dielectric layer on the light outcoupling efficiency of the top emitting orgainic light-emitting devices (OLEDs) is analyzed. A combined evaluation followed by detailed design and optimization is proposed and described in detail. The analysis shows that this cladding layer affects the device's outcoupling efficiency with three different extents as the thickness of the metal layer in the multilayer cathode varying. The simulation results give a reasonable agreement with former experiment results.

OCIS codes: 230.3670, 230.4170, 310.6860, 140.4780.

In recent years, top emitting organic light-emitting devices (OLEDs) with dual-metal-mirror microcavity structures have attracted more attention[1−3] due to their advantages over the conventional bottom emitting structures[4,5]. Recently a novel structure with a dielectric cladding layer on the cathodes to improve the light extraction efficiency is proposed and experimentally studied[6]. As this cladding layer is designed, however, the calculated results only from the consideration of thin film optics may excessively disagree with those from experiments. This total difference may come from electrical and optical aspects. Nevertheless, the electrical performance can be optimized to ensure little difference between the design and the experiments[6]. Hence this wide gap between theoretical design and experiments should be caused by the optical property, while to our knowledge, little research in this aspect has been made so far. In this letter, we propose a combined analysis and design method to optimize this cladding layer with respect to the microcavity effect as well as the potential transmittance. The basic dual-metal-mirror structure used in our analysis is shown in Fig. 1. A thin emission layer and the related parameters used in our simulation are also demonstrated in this figure. The semitransparent metal thin film is a part of the multilayer cathode and used for electron injection. Two sides of the metal film are an organic layer and the cladding dielectric layer, respectively. Taking account of the little difference in refractive indices of most organic materials used in OLEDs for different functions, we apply the single organic layer approximation in our study for generality. The thickness of anode metal layer is assumed thick enough and treated as a bulk material. In Fig. 1, $r_{e,\mathrm{Fw}}$ and $r_{e,\mathrm{Bw}}$ represent the reflection coefficients at the front and the rear interface of the microcavity, respectively. y_{anode}, y_{cathode}, n_{air}, and n_{clad} are the reflective indices of the anode metal layer, cathode metal film, air, and the cladding layer, respectively; z_{Fw} is the distance from the emitting dipole to the front interface, and z_{Bw} is that to the rear interface; d_e is the thickness of the organic layer. We should point out that generally this cladding layer only work within a limited emission wavelength region, so we may focus on a single wavelength ($\lambda = 550$ nm) for simplicity.

Firstly we consider the complex multilayer cathode as a film stack which contains a thin metal film. The organic layer and air are assumed as half-infinite incident and exit media, respectively. Hence the whole film system, organic|metal|dielectric|air, can be analyzed and calculated through character matrix[7]. Thus the potential transmittance of the metal-dielectric film stack, defined as

$$\psi = \frac{T}{1-R}, \tag{1}$$

should be used to describe the transmission ability of the film system for the case that there exists absorption in the metal film. Known from the optics of thin films, the maximum potential transmittance $\psi_{\max}$ is only the function of the complex refractive index and the thickness of the metal film, and they can be easily derived from matrix formula[7]. Then optimum admittances of the incident and exit media can also be determined, which ensure that $T = \psi$. When only a single "dielectric" layer is employed as a capping layer on the metal electrode to approach $\psi_{\max}$, we can obtain

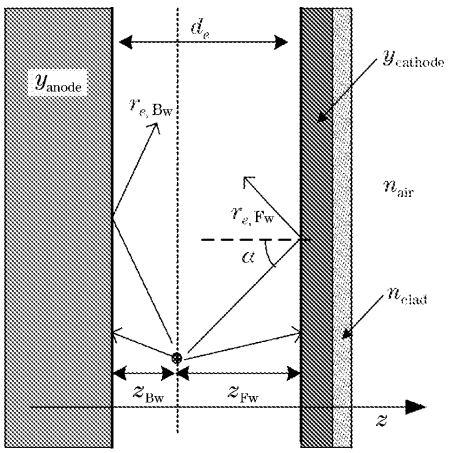

Fig. 1. Schematic illustration of the OLED microcavity structure used in the analysis.

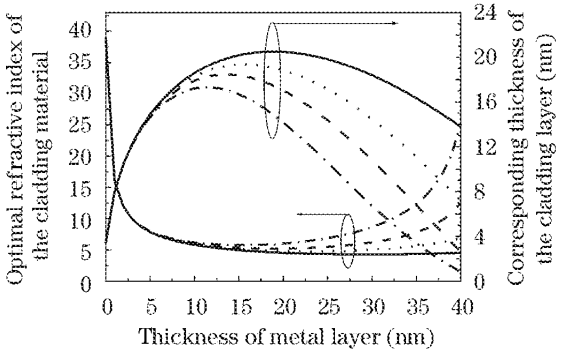

Fig. 2. The calculated optimal refractive index and thickness of the cladding layer with different thickness of the metal layer. The metal materials are Ca (solid line), Mg (dotted line), Ag (dashed line), and Al (dash-dot line).

Table 1. Material Parameters Used in the Calculation

Metal	n	k
Ca[8]	0.620	2.14
Mg[8]	0.370	4.42
Ag[9]	0.055	3.32
Al[8]	0.820	5.99
Au[9]	0.330	2.82

$$\begin{cases} \delta_d = m\pi + \arctan\left[\frac{(X_{\rm opt}-1)n_d}{Z_{\rm opt}}\right] \\ n_d = \left(\frac{Z_{\rm opt}^2}{X_{\rm opt}-1} + X_{\rm opt}\right)^{1/2} \end{cases} \quad (2)$$

where $m = 0, \pm 1, \cdots$, δ_d and n_d are the phase and the refractive index of this layer, respectively. $X_{\rm opt}$ and $Z_{\rm opt}$ are the real and imaginary part of the optimum admittance of the exit medium, respectively. According to δ_d we can get the minimum thickness of the layer. Assuming calcium, magnesium, aluminum, and silver as the metal electrode, these two parameters are estimated, as shown in Fig. 2. The thickness of the metal layer is restricted within 40 nm in the simulation and the differences of refractive indices due to their thickness variance are neglected for simplicity. The material parameters used in the calculation are listed in Table 1. According to the evaluation, the lowest necessary refractive index of the "dielectrics" is about 4.8. There is no natural dielectric material matching it and the most approaching value is only 2.4. Hence this single-cladding-layer structure cannot induce the maximum potential transmittance due to its intrinsic characteristics. We also evaluate the potential transmittance and the critical angle $\theta_{\rm cr}$ numerically. According to the result, little difference exists between the transmittance of oblique incidence on the complex cathode and that of normal incidence when the incident angle less than $\pm 20°$, and the separation of the spectra between TE- and TM-mode waves is also neglectable. In our case the critical angle is about 30° so that the potential transmittance decreases to zero acutely as the incident angle approaches the critical angle.

So far, however, we have only considered one side of the problem. Noting that the enhancement factor of microcavities is strongly dependent on the reflectance, we should investigate the whole effects of this cladding dielectric layer in this improved structure, including the variance of the emission power in the microcavity. Here we propose a combined parameter P to describe the total power outcoupling ability of the device

$$P = \psi \cdot M_{\rm cav}, \quad (3a)$$

and

$$M_{\rm cav} = \int_0^\infty |C^{\rm TE,TM}| \left\{ {\rm Re}\left[\frac{(1 \pm r_{e,{\rm Fw}}^{\rm TE,TM} {\rm e}^{(2ik_{e,z}z_{\rm Fw})})(1 \pm r_{e,{\rm Bw}}^{\rm TE,TM} {\rm e}^{(2ik_{e,z}z_{\rm Bw})})}{1 - r_{e,{\rm Fw}}^{\rm TE,TM} r_{e,{\rm Bw}}^{\rm TE,TM} {\rm e}^{(2ik_{e,z}d_e)}} \right] \right\}^2 \times {\rm d}\kappa^2, \quad (3b)$$

where $\kappa = k \sin\alpha$, $k_{e,z}$ is the normal part of the wave vector in organic layer, and other symbols used here have been explained above. In Eq. (3a), ψ is the potential transmittance, and $M_{\rm cav}$ represents the total spontaneous emission power in the microcavity modified by the detailed cavity structure[10]. Using this combined model, we can completely evaluate the effect of the cladding layer on the light outcoupling efficiency and obtain the optimal thickness of this dielectric layer. In our simulated configuration, a magnesium film of varying thickness serves as the cathode, and the anode is 90-nm-thick gold layer. The thickness of the microcavity is 130 nm and the refractive index $n = 1.7$. According to the above analysis, we assume the refractive index of the cladding layer is 2.4. This structure is similar to that proposed in former

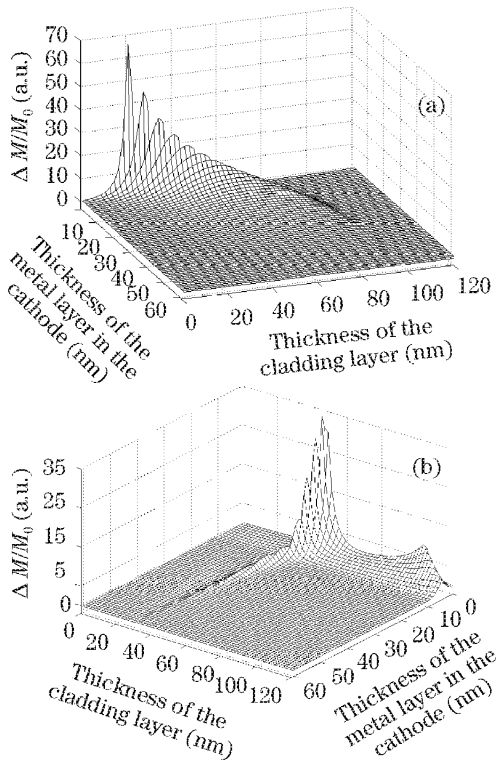

Fig. 3. Normalized variance of the radiation power ($\Delta M/M_0$) of TE mode (a) and TM mode (b) in the microcavity.

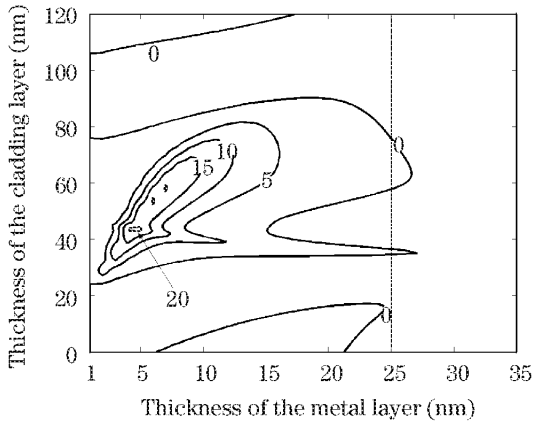

Fig. 4. Variance of P within about one thickness period, normalized with $(P - P_0)/P_0$, P_0 is the reference value obtained without the cladding layer.

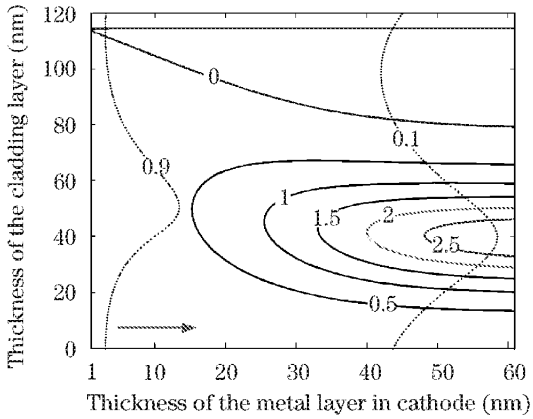

Fig. 5. Variance of ψ within about one thickness period, normalized by $(\psi - \psi_0)/\psi_0$, ψ_0 is the reference value obtained without the cladding layer. The dotted lines represent the potential transmittance values and the arrow shows the direction in which ψ decreases from 90% to zero.

experiment[6]. In Fig. 3 the relative variance of radiation power ΔM of TE and TM modes in the cavity with reference to the power M_0 obtained without the cladding layer are shown respectively, which have been normalized by M_0 , and the final performance of P is shown in Fig. 4.

For clearly understanding the physical implication of P and the whole effect of the cladding dielectric layer on the light outcoupling performance, we give the relative variance of ψnormalized by the value calculated without the cladding layer, as shown in Fig. 5. Based on Fig. 4, combining Figs. 3 and 5, one can find there exist three regions exhibiting different optical performance with the increase of the metal layer's thickness in this multilayer cathode. When the metal layer is thinner than 15 nm, the increasing thickness of the dielectric layer will strongly modify the microcavity's enhancement factor $M_{\rm cav}$ and then P even though the fluctuation of ψ is small. As the thickness of this dielectric layer increases more (but still less than 30 nm), the fluctuation of ψ enhances gradually whereas $M_{\rm cav}$ lowers. Therefore the final superposition results in less effect on the total outcoupling efficiency. If the metal layer's thickness continues increasing, the variance of P will vanish, because the variance magnitudes of ψ and $M_{\rm cav}$ (Fig. 3) are nearly zero though in this region the fluctuation of ψ becomes more intensive.

In addition, considering the similarity between this optimized structure and that proposed in former experiment[6], we can give a reasonable explanation about that result. As the dotted line in Fig. 4, when the cathode metal layer is around 25 nm thick, there are two thickness ranges of the cladding layer corresponding to the outcoupling enhancement, one is near 38 nm, and the other is 55 – 70 nm. Practically the enhancement factor of the latter region is about 2 times of that of the former and it is easier to be detected. This shows a reasonable agreement with the experiment.

In conclusion, we have detailedly discussed the optimal thickness and refractive index of the dielectric cladding capping on the dual-metal-mirror microcavity structure of the top emitting OLEDs, and analyzed the effect of the cladding on the device's light outcoupling performance. This analysis and optimization procedure can also be extended to other OLEDs with similar microcavity structures.

L. Yang's e-mail address is yanglig@zju.edu.cn.

References

1. M. H. Lu, M. S. Weaver, T. X. Zhou, M. Rothman, R. C. Kwong, M. Hack, and J. J. Brown, Appl. Phys. Lett. **81,** 3921 (2002).
2. S. Han, X. Feng, Z. H. Lu, D. Johnson, and R. Wood, Appl. Phys. Lett. **82,** 2715 (2003).
3. T. Dobbertin, M. Kroeger, D. Heithecker, D. Schneider, D. Metzdorf, H. Neuner, E. Becker, H.-H. Johannes, and W. Kowalsky, Appl. Phys. Lett. **82,** 284 (2003).
4. P. A. Hobson, J. A. E. Wasey, I. Sage, and W. L. Barnes, IEEE J. Sel. Top. Quantum Electron. **8,** 378 (2002).
5. L. S. Hung, C. W. Tang, M. G. Mason, P. Raychaudhuri, and J. Madathil, Appl. Phys. Lett. **78,** 544 (2001).
6. H. Riel, S. Karg, T. Beierlein, B. Ruhstaller, and W. Riess, Appl. Phys. Lett. **82,** 466 (2003).
7. H. A. Macleod, *Thin-Film Optical Filters* (2nd edition) (Adam Hilger, Bristol, 1986) p. 295.
8. G. Hass and L Hadley, *American Institute of Physics Handbook* (McGraw Hill Book Company, New York and London, 1972) p. 6.124.
9. E. D. Palik, *Handbook of Optical Constants of Solids* (Academic Press Inc., San Diego and London, 1985) p. 250.
10. K. A. Neyts, J. Opt. Soc. Am. A **15,** 962 (1998).